agronomy

MDPI

Article

Influence of Pre-Hydrolysis on the Chemical Composition of *Prunus avium* Cherry Seeds

Luísa Cruz-Lopes [1,*], Yuliya Dulyanska [1], Idalina Domingos [1], José Ferreira [1], Anabela Fragata [2], Raquel Guiné [1] and Bruno Esteves [1]

[1] CERNAS Research Centre, Polytechnic Institute of Viseu, 3504-510 Viseu, Portugal; yuliyadulyanska@esav.ipv.pt (Y.D.); ijd@estgv.ipv.pt (I.D.); jvf@estgv.ipv.pt (J.F.); raquelguine@esav.ipv.pt (R.G.); bruno@estgv.ipv.pt (B.E.)

[2] CI&DEI Research Centre, Polytechnic Institute of Viseu, 3504-510 Viseu, Portugal; afragata@estgl.ipv.pt

* Correspondence: lvalente@estgv.ipv.pt; Tel.: +351-232-480-500

Abstract: During the industrial processing of sweet cherry fruits, the seeds are considered agricultural waste and must be disposed of, typically through burning. In this context, it is intended to contribute to the scientific development of the ecovalorization of by-products and to provide new strategies for their transformation into value-added products obtained from sweet cherry seeds (SCS). This work aimed to establish the chemical characterization of SCS before and after several pre-hydrolysis steps in order to allow the solubilization of hemicelluloses that can later be used for the recovery of sugars. The higher percentage of cellulose and lignin remaining in the solid phase will allow its further processing for an integral valorization of the raw material. The temperature (160 and 170 °C) and time (0 and 180 min) of pre-hydrolysis were optimized to obtain the best liquefaction. The percentage of liquefied material was determined from the solid waste obtained at the time of filtration. The best liquefaction by the hydrolysis of SCS was obtained at 170 °C and 180 min, with a yield of 26.7%. The chemical analyses of SCS throughout hydrolysis showed the solubilization of hemicelluloses with increases in the time and temperature of the reactor. α-cellulose and lignin showed an increase both with temperature and time, increasing the material's potential for further processing in adhesives. FTIR analysis showed that there were significant changes in the spectra between the initial SCS, the solid residue, and the liquefied material. Pre-hydrolysis was proven to be an efficient process to improve the chemical composition of the material for further processing into adhesives or higher-mechanical-strength polyurethane foams.

Keywords: sweet cherry seeds; *Prunus avium* L.; chemical composition; pre-hydrolysis; ecovalorization; agro-industrial residues

check for updates

Citation: Cruz-Lopes, L.; Dulyanska, Y.; Domingos, I.; Ferreira, J.; Fragata, A.; Guiné, R.; Esteves, B. Influence of Pre-Hydrolysis on the Chemical Composition of *Prunus avium* Cherry Seeds. *Agronomy* **2022**, *12*, 280. https://doi.org/10.3390/agronomy12020280

Academic Editor: Jose Maria Barrero

Received: 23 December 2021
Accepted: 18 January 2022
Published: 21 January 2022

Publisher's Note: MDPI stays neutral with regard to jurisdictional claims in published maps and institutional affiliations.

Copyright: © 2022 by the authors. Licensee MDPI, Basel, Switzerland. This article is an open access article distributed under the terms and conditions of the Creative Commons Attribution (CC BY) license (https://creativecommons.org/licenses/by/4.0/).

1. Introduction

Sweet cherry, or *Prunus avium* L., is one of the most popular fruit of the *Rosaceae* family, *Prunoideae* subfamily, and *Prunus genus*, which have their origin in the Western Asian continent. Sweet cherry (*Prunus avium* L.) is the most cultivated species [1], and this popularity is based on its high appreciation by consumers due to its excellent quality [2]. The annual global sweet cherry production is around 2.2 million tons. The main sweet cherry producer in 2020/2021 concerning different countries was Turkey (23.4%), followed by the European Union (17.9%), United States (9.8%), China (11.5%), Ukraine, and Chile (7.7% and 7.3%, respectively) [3]. Portugal's climatic conditions have allowed the cherry tree to adapt very well, making its cultivation viable in various regions of the country. Studies conducted by the INE [4] (Portuguese Bureau of Statistics) showed that the Portuguese sweet cherry industry has an implementation area of 6387 ha, producing 9241 t of this fruit. Its production extends mainly through three regions: the North (area of 3177 ha and production of 6586 t), Centre (area of 3099 ha and production of 2510 t), and Alentejo (area

of 64 ha and production of 57 t) [5]. There are several varieties of cherry in Portugal. The most important traditionally cultivated cherries are: De Saco da Cova da Beira, De Saco do Douro, Lisboeta, São Julião, Big Burlat, Maring, Napoleon Pé Comprido, and Big Windsor, and the first four cherries are of national origin [6]. Research shows that particular interest has focused not only on the nutritional value of this fruit, but also on its high health benefits due to its content of bioactive compounds, such as its antioxidant, anti-inflammatory, and anticancer properties [7–9].

When some fruits are processed by industry, wastes are inevitably produced. The seeds of the sweet cherry are not used for food and are generally considered agricultural waste by the processing industry, and must be disposed of, typically through burning. Thus, seed removal and disposal substantially raise production costs and contribute to pollution [10]. This has contributed to the increased research on this topic, addressing the possible uses of these residues to obtain high-value products in order to reduce environmental management costs [11]. Residues are also often used in composting processes [12]. Similarly to sour cherry, sweet cherry seeds are composed of two parts: the shell that corresponds to 75–80% in sour cherries and the kernel that represents the remainder (20–25%) [13]. According to these authors, the shell is used almost exclusively as fuel or considered waste. The kernel, however, is used for oil extraction. There have been some studies on sweet cherry seed oil, which, according to Bernardo-Gil et al. [14], contains more than 87% unsaturated fatty acids, such as oleic acid (43.7% by weight) and linoleic acid (41.8% by weight). New uses for sweet cherry seeds, mainly for their shell portion, are, therefore, of the utmost importance. There is a lack of knowledge on the chemical composition of sweet cherry seed shells and the overall composition of the seed. Results presented previously show that the main components of sweet cherry seeds are lignin, cellulose, and hemicelluloses [15–18].

Structural components are parts of cells; they are macromolecules of a polymeric nature, and this type of component includes cellulose, hemicelluloses, and lignin. Cellulose is a linear homopolymer formed by n repeated D-glucose units bound by β-1.4 glycolipid bonds (n 10 $\geq$ 000). The glucose units are connected to each other by Van der Waals forces and hydrogen bonds [12].

Hemicelluloses are heterogeneous polysaccharides consisting of a mixture of pentoses (D-xylose and D-arabinose), hexoses (D-glucose, D-galactose, and D-mannose), and some hexuronic acids in small amounts, such as D-galacturonic acid, D-glucuronic acid, and its acid derivative 4-O-methylglucuronic acid [19]. In hemicellulose, the degree of polymerization ($50 \leq n \leq 300$) is lower than that in cellulose ($n \geq 10{,}000$), and hemicellulose is ramified and amorphous; therefore, it is less resistant to chemical degradation [20]. Unlike hemicelluloses, cellulose is linear and contains amorphous and crystalline zones [19].

Lignin is the second most abundant biopolymer in biomass after cellulose; it is a very complex and branched aromatic biopolymer [20]. The helical structure of lignin mainly results from the polymerization of three phenylpropanoid monomeric units: p-coumaryl alcohol, coniferyl alcohol, and sinapyl alcohol [20,21]. These phenylpropanoids give rise to the following phenolic substructures: p-hydroxyphenyl (H); guaiacyl (G) and syringyl (S), respectively [21]. Lignin has been used for the production of polyurethane foams and adhesives. Some authors state that the compression strength of PU foams increases with their lignin content [22,23]. Others state that, although the compressive properties of rigid polyurethane foams increase in the direction of foam rise with higher amounts of Kraft lignin, they decrease in the perpendicular direction [24]. Several authors reported higher hydrophobicity and flame retardancy with higher KL content [23,25,26], but also increased brittleness [23]. Adhesives from lignin have been studied for several years [27–32] and some authors have even stated that these adhesives can have a similar performance to phenol-formaldehyde resins [29]

There are mainly three different types of pre-hydrolysis: acid pre-hydrolysis, auto- pre-hydrolysis, and alkaline pre-hydrolysis. In accordance with Hamaguchi et al. [33], acid pre-hydrolysis, usually using sulfuric acid as a catalyst, leads to the production of oligomeric and monomeric sugars. Some authors, however, mention that acid pre-hydrolysis has corrosive

effects on equipment and, at the same time, promotes extensive lignin condensation, and even a low yield due to some undesirable cellulose hydrolysis [34]. Auto hydrolysis is also a process under acidic conditions due to the acetic acid released by the cleavage of acetyl groups in hemicelluloses. Alkaline pre-hydrolysis is generally conducted with green or white liquor from the kraft process with strongly alkaline solutions under low temperatures [33,35,36]. Mechanical pre-treatment has also been used, generally to prepare samples for enzymatic or chemical hydrolysis with the objective to reduce the particle size and cellulose crystallinity so that enzymes or chemicals have better access [19,20,37,38]

Pre-hydrolysis with water (auto-hydrolysis) is the most used pre-treatment, in which biomass is subjected to compressed hot water, enabling the extensive solubilization of hemicelluloses [10]. The main reaction in this step is the depolymerization of hemicelluloses, leading to the formation of sugars and oligosaccharides [39,40]. The reaction is catalysed by hydronium ions resulting from water autoionization and in situ-generated organic acids. These acids act as a catalyst to hydrolyse the glycosidic bonds in hemicelluloses that are depolymerized into low-molecular-weight polysaccharides, oligosaccharides, monosaccharides, and other products, such as furfural and hydroxymethylfurfural. Due to the acid that is also released, some lignin and acetic acid can be found in the hydrolysate [26]. Additionally, pre-hydrolysis increases the surface area and decreases the crystallinity of cellulose, resulting in improved susceptibility towards future hydrolysis. Some authors state that pre-hydrolysis is a dynamic process, where, due to the acids released, the amount of hemicelluloses removed by acid hydrolysis in this process increases over time. However, at the same time, part of the obtained xylose is converted into furfural [41]. Therefore, the pre-hydrolysis time and temperature must be optimized to obtain the maximum amount of sugar without significant furfural conversion.

This work aims to establish the chemical characterization of sweet cherry seeds before and during the pre-hydrolysis of sweet cherry seeds, also aiming at obtaining an enriched lignin material that can be further processed into value-added products, such as adhesives.

2. Materials and Methods

2.1. Materials

The sweet cherry seeds (SCS) used in this study were wastes produced by the company Nutrofertil based in Portugal (Tondela), which is a residue management company. The samples were milled in a Retsch SMI mill (Retsch GmbH, Haan, Germany) and sieved using a Retsch AS200 (Retsch GmbH, Haan, Germany) for 20 min at 50 rpm. Four fractions, >40 mesh, 40–60 mesh, 60–80 mesh, and <80 mesh were obtained, but only the 40–60 mesh fraction was used for the tests.

2.2. Chemical Composition

The SCS were characterized for their ash content, extractives (in dichloromethane, ethanol, and hot water), α-cellulose, lignin, and hemicelluloses, Figure 1.

The 40–60 mesh fraction was dried at 105 °C for at least 24 h and afterwards used for the chemical analyses according to Tappi T 264 om-97 [42]. The average chemical composition of each sample was determined in triplicate. The extractives were determined by extraction with different solvents in sequential order of ascending polarity.

The ash content was determined by the calcination of the material at 525 °C according to the standard procedure Tappi T 211 om-93 [43]. The inorganic composition was determined by ICP after ash wet digestion in a Leco CHNS-932 Elemental Analyzer (St. Joseph, MI, USA). The extractive content consisted of the determination of dichloromethane, ethanol, and hot water extractives using Soxhlet extraction according to Tappi T 204 om-88 [44] as follows: approximately 10 g of the dried sample was used for Soxhlet extraction using 150 mL of dichloromethane, ethanol, and water as solvents. The extraction time was 6 h for dichloromethane and 16 h for ethanol and water, respecting a sequential extraction with increasing polarity. The extractive content was determined in relation to the dry material.

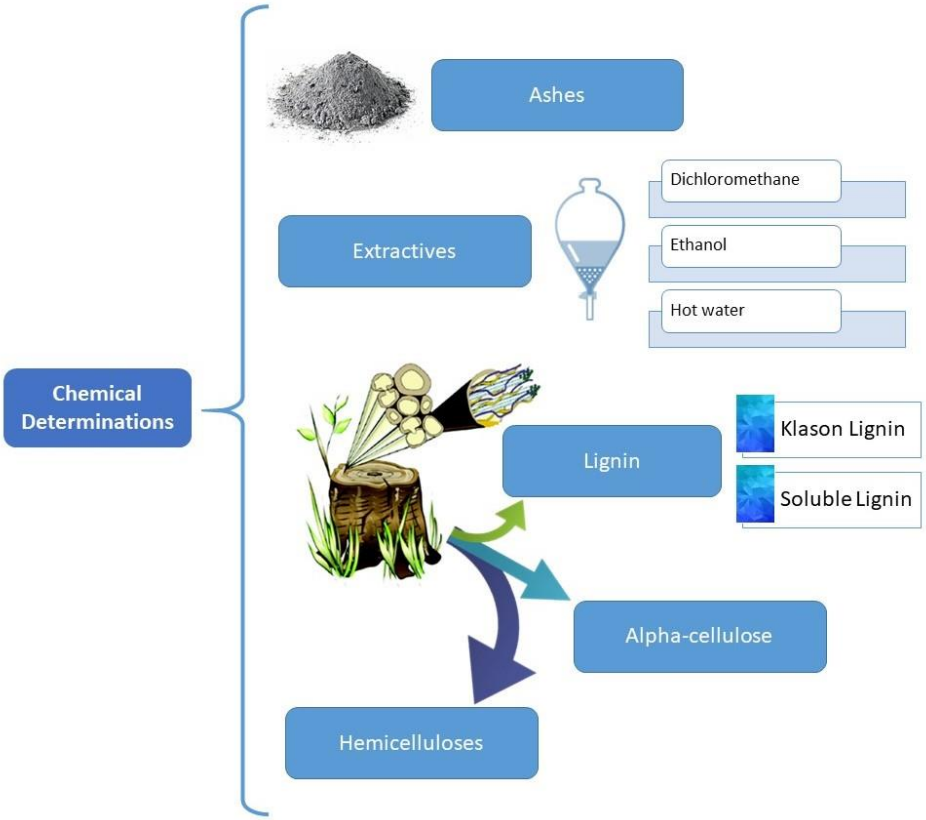

Figure 1. Scheme of the determination of the chemical composition of SCS.

The lignin content in SCS free of extractives was determined by the *Klason* method with 72% H_2SO_4 (according to Tappi T 204 om-88) [45]. The method consisted of two hydrolyses. The first hydrolysis was performed with 72% H_2SO_4 for 1 h, and the second with 3% H_2SO_4 in an autoclave at 120 °C for 1 h. The insoluble residue was obtained by filtering in a G2 glass crucible, and then dried to a constant weight. Then, the soluble lignin was analysed through spectrophotometry by measuring the absorption at 205 nm.

Holocellulose was determined by the acid chloride method in a water bath at 70 °C until the sample became white. The insoluble material was then filtered and dried [46]. The α-cellulose content was determined by hydrolysing the holocellulose with 2.5 mL of 17.5% NaOH in a thermal bath. The insoluble residue was filtered, washed with 8.3% NaOH and distilled water, finishing with 3.75 mL CH_3COOH 10% in a G2 glass crucible, and dried to a constant weight. The hemicellulose content was determined by the difference.

2.3. FTIR Analysis

The Fourier transform infrared spectroscopy (FTIR) technique was used to evaluate the functional groups present in the original sample of SCS and the sample that underwent pre-hydrolysis.

The initial dried SCS, the liquefied material, and the resulting solid residue were analysed by FTIR-ATR. The samples were previously crushed and dried in an oven at 100 °C for one week in order to ensure that water was completely removed.

FTIR-ATR spectra were taken using a Perkin Elmer UATR Spectrum Two (Waltham, MA, USA) with 72 scans/min and a resolution of 4.0 cm^{-1} over the 4000 to 400 cm^{-1} range. After performing the background, the sample was placed over the crystal. Solid samples were pressed against the crystal. An average of three spectra was used.

2.4. Pre-Hydrolysis

Pre-hydrolysis was carried out in a PARR LKT PED cylindrical glass reactor of 600 mL with a double coating. A 20 g sample (60 mesh) and 200 mL of distilled water were introduced into the reactor, and the automatic stirrer was set at 70 rpm. The temperature (160 and 170 °C, oil temperature on the shirt) and time (30, 60, 90, and 180 min) were optimized to obtain the best liquefaction percentage. After removal from the reactor, the mixture was filtered through a Buckner funnel with a paper filter, and the solid residue was separated from the liquefied fraction, oven dried, and weighed. The percentage of liquefied material was determined in accordance with Equation (1).

$$Liquefaction\ Yield\ (\%) = \frac{Initial\ dry\ mass\ (g) - Solid\ dry\ residue\ (g)}{Initial\ dry\ mass\ (g)} \times 100$$

To determine the chemical composition of the solid fraction, dried material was used, and the content of the following components was determined: Klason Lignin, holocellulose, α-cellulose, and hemicelluloses, using the 40–60 mesh fraction. The extractives were assumed to be mostly removed during pre-hydrolysis.

3. Results and Discussion

3.1. Chemical Composition

Table 1 presents the chemical composition of the SCS, where it can be observed that it was composed of 1.31% ashes, while total extractives represented around 4.69%, most of which were soluble in water (2.14%) and ethanol (2.04%), and only 0.49% in dichloromethane. The total lignin was 32.94%, most of which was insoluble lignin (31.67%) and the remaining 1.27% was soluble. α-Cellulose had a value of about 23.10% and 37.96% for hemicelluloses. The determination of the chemical composition will allow us to better understand the possible uses of SCS.

Table 1. Chemical composition of SCS.

Parameters		Content (% Dry Matter, *w*/*w*)
Ashes		1.31
	Na	0.10
	Mg	0.58
	P	0.95
	K	3.2
	Ca	0.93
	Fe	0.02
	Zn	<0.01
	Dichloromethane	0.49
Extractives	Ethanol	2.04
	Hot water	2.16
	Total	4.69
Lignin	Soluble	1.27
	Insoluble (*Klason*)	31.67
α-Cellulose		23.10
Hemicelluloses		37.96

Although the value obtained for the ashes (1.31%) is higher than the values obtained for SCS by Venegaz-Gomez et al. [47], Duman et al. [15], and Kamel et al. [48], with 0.24%, 1.16%, and 1.2%, respectively, the differences are not significant. The inorganic composition shows that SCS are more rich in potassium, with 3.2%, than all the other constituents, followed by calcium (Ca) and phosphorous (P), with 0.93 and 0.95%, respectively. There was also approximately 0.6% of magnesium (Mg) and a smaller amount of sodium (Na, 0.1%). Potassium was also the most representative element in grape stalks, followed by calcium, magnesium, zinc, and sodium [44]. Comparing the inorganic composition with those of black cherry seeds, almonds, and peanuts, all of these materials have higher

percentages of potassium, followed by phosphorous; however, the third most representative mineral was magnesium, followed by calcium, with the exception of almonds, in which these inorganic compounds had the opposite order. Sodium and iron also had the lowest contents, similar to SCS [49].

Relative to hemicellulose in the present study, the value of 37.96% is higher compared with that in the studies by Gonzalez et al. [50], with 14.7%, and Duman et al. [15], with 28.59%. Nevertheless, these authors did not present the method used in their studies. The cellulose content was lower than the values obtained by Petrov et al. [16] and Gonzalez et al. [17], with 30% and 29.4%, respectively. The Klason lignin content is similar to the results obtained by Gonzalez et al. [50], González-Domínguez et al. [18] (30.7%), and Duman et al. [15] (29.08%), but lower than the results obtained by Petrov et al. [16] (40%).

Pre-hydrolysis with water (auto-hydrolysis) is an excellent method to remove hemicelluloses from lignocellulosic materials by a simple process without using chemical compounds. In order to optimize the liquefaction conditions of the pre-hydrolysis, tests were performed at different times (between 30 and 120 min) and temperatures of 160 °C and 170 °C. The results are presented in Figure 2, where it can be seen that the liquefaction yield increased with the temperature and time of the process. For example, using a temperature of 160 °C, the liquefied yield was around 6.3% for a 30 min liquefaction time, but it increased to 18.6% for 180 min. Similarly, at 170 °C, the liquefied yield for 180 min was about 26.6%, much higher than that obtained at 160 °C. A higher temperature might lead to better liquefaction percentages; however, some authors stated that 170°C was the optimum temperature to remove hemicelluloses without significant conversion of xylose to furfural [41]. The liquefaction percentages are higher than those obtained, for example, in the auto-hydrolysis of *Eucalyptus globulus* wood at 150 °C for 3 h (12.5%) [50] or *Eucalyptus urograndis* (10.8%) at 165 °C for 0.5 h [51]. Al-Dajani et al. obtained 19% liquefaction for aspen wood by auto-hydrolysis at 150 °C for 4.5 h [52].

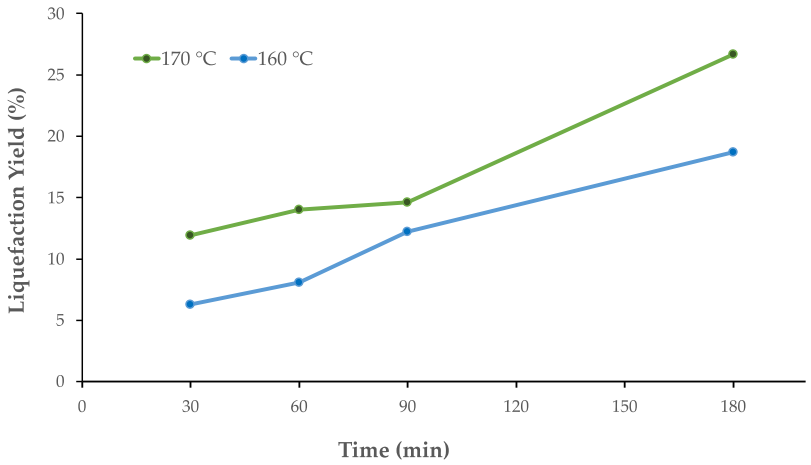

Figure 2. Pre-hydrolysis of SCS. Liquefaction yield with time.

Figure 3 presents the chemical composition variation over the several pre-hydrolysis steps at both temperatures of 160 °C and 170 °C.

For α-cellulose, the values obtained for the two temperatures are very different. There is a significant increase in α-cellulose from 23.1% in the original sample to 39.1% at 170 °C, but only a moderate increase at 160 °C to 27.4%. The increase in α-cellulose shows that this polymer is the most resistant to the pre-hydrolysis process, at least the crystalline part of the cellulose, since α-cellulose mostly represents this part. The reduction of hemicelluloses might even be higher since the solubilized cellulose counts toward the hemicellulose content.

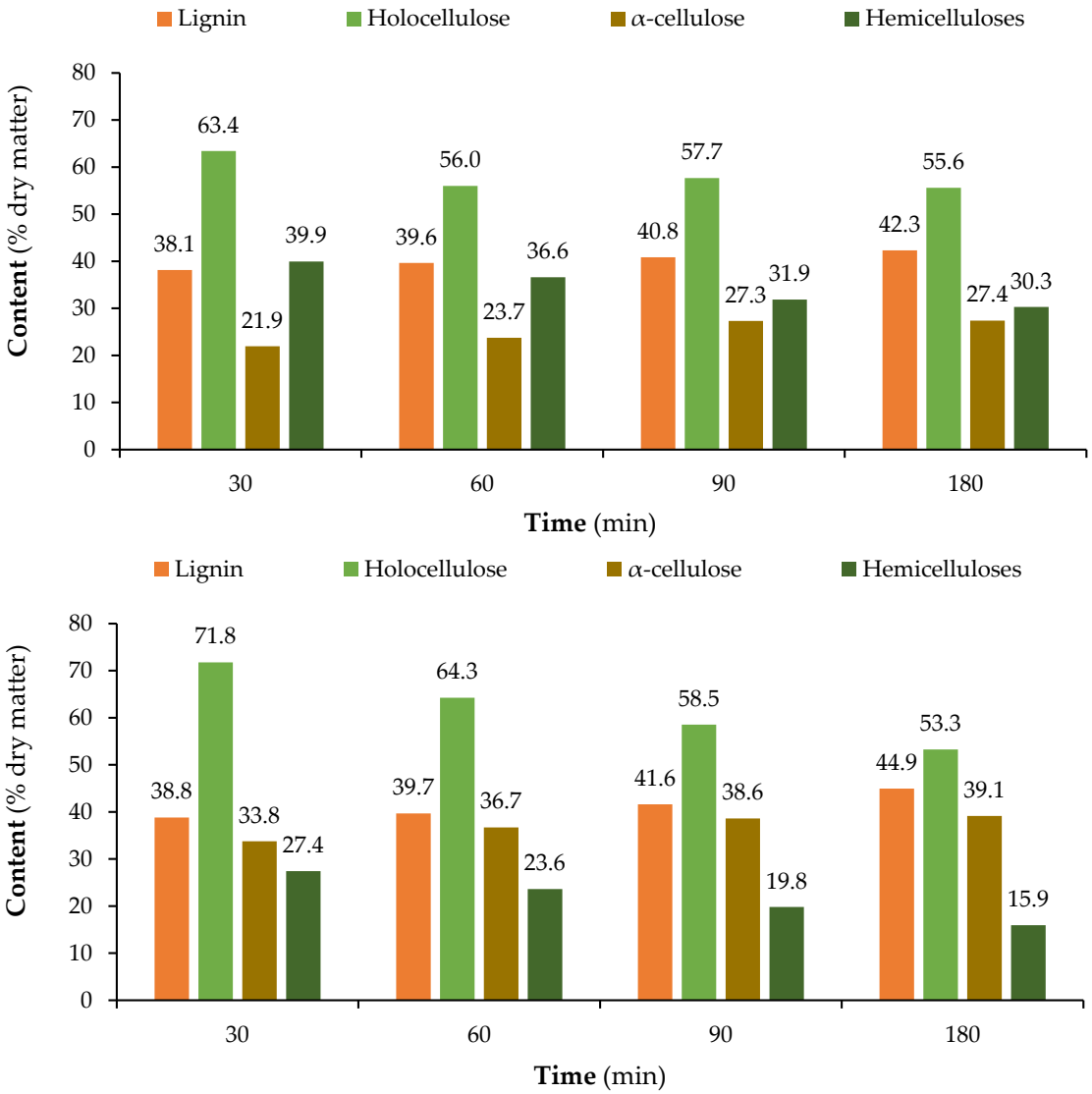

Figure 3. Variation in the chemical composition of the hydrolysed SCS with time at 160 °C (**top**) and 170 °C (**bottom**).

The influence of pre-hydrolysis temperature is better seen in Figure 4, where the differences between the initial material and solid residue after pre-hydrolysis are clearer, being expressed as a percentage of the initial content for each component. The hemicellulose content decreased to only 80% of the initial content at 160 °C, and even further to only 42% at 170 °C. On the other hand, the lignin and α-cellulose contents increased; particularly, the latter increased to 169% of the original value when treated at 170 °C. Holocellulose also decreased, and its reduction was lower than the relative increase in α-cellulose for both temperatures.

It was further observed that both the reaction time (Figure 3) and temperature (Figure 4) had a significant effect on the decrease in the hemicellulose content.

3.2. FTIR-ATR Analysis

FTIR-ATR of the SCS and of the liquefied and solid residues over the several pre-hydrolysis steps were performed. Figure 5 presents the spectra of the initial SCS and of the residue obtained after pre-hydrolysis at 160 °C and for a 30–180 min reaction time. The most characteristic peaks are marked for readability purposes.

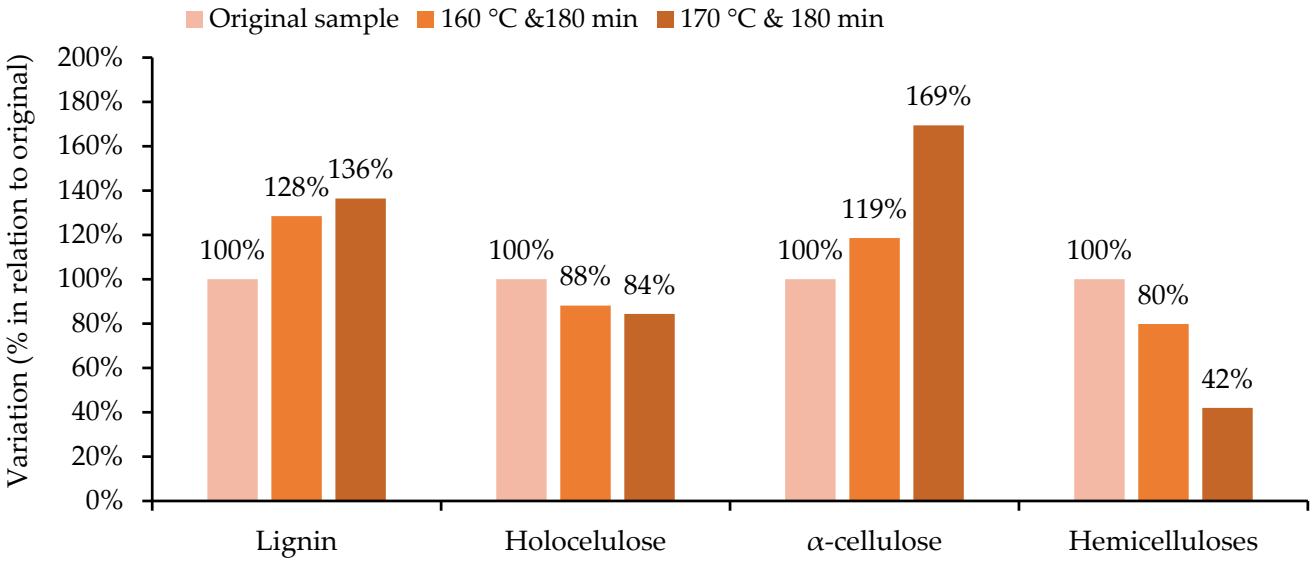

Figure 4. Variation in the chemical composition of the SCS hydrolysed in relation to the original sample, depending on the temperature at the end of the process (time of 180 min).

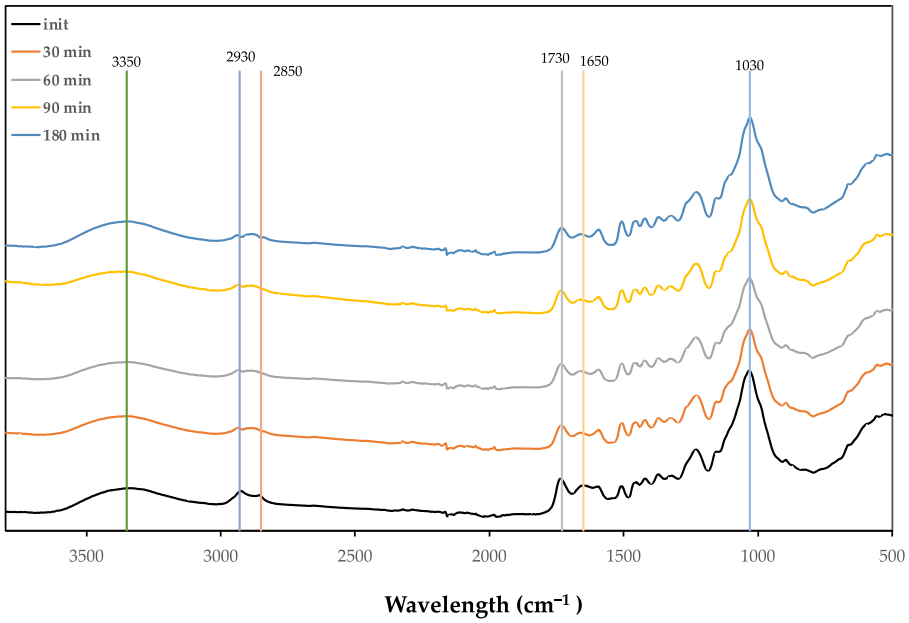

Figure 5. FTIR spectra of the original and solid residue from hydrolysed SCS at 160 °C.

Comparing the initial material with the residue, there seems to be a slight decrease and a narrowing of the OH band around 3350 cm^{-1}. The peaks at 2930 cm^{-1} and 2850 cm^{-1} have different behaviours. There is a decrease in the peak at 2930 cm^{-1} that becomes less distinguished from the peak at 2850 cm^{-1}. With the prolongation of the reaction time, this region divides into three different peaks, around 2930 cm^{-1}, 2885 cm^{-1}, and 2850 cm^{-1}. These bands are composed of the stretching asymmetric vibrations of -CH_3 (2970–2950 cm^{-1}) and -CH_2- (2935–2915 cm^{-1}) and stretching symmetric vibrations of -CH_3 (2880–2860 cm^{-1}) and -CH_2- (2865–2845 cm^{-1}) [53]. Usually, the asymmetric band is higher, which was true for the initial material but changed throughout the pre-hydrolysis treatment. This shows that there were some changes in the neighbourhoods of these bands. One of the possible reasons is the relative increase in the methoxyl groups in lignin due to the reduction of carbohydrates, since the CH_3 stretching vibrations of methoxyl have lower frequencies [54,55].

The bands at 1730 cm^{-1} and 1650 cm^{-1} were attributed to non-conjugated and conjugated C=O bonds. There seems to be a decrease specifically in the 1650 cm^{-1} peak. Lignin has been mentioned to have high absorption at 1600 cm^{-1} due to benzene ring stretching vibrations, but at this wavenumber there seemed to be no differences between the original material and the solid residue. No significant changes could be observed in the fingerprint region, although there seems to be a slight increase in the 1500 cm^{-1} peak. There is a decrease in the peak at 1360 cm^{-1} in relation to the peak at 1330 cm^{-1}.

There is also the appearance of a shoulder at around 1130 cm^{-1} that seems to be due to the slight narrowing of the 1030 cm^{-1} band. This might be due to the decreased absorption at around 1100 cm^{-1}, which was attributed to the C-O stretching vibrations in carbohydrates. At 170 °C, the changes in the spectrum are similar to those observed for 160 °C, with a slight decrease in the OH band and a decrease at 1650 cm^{-1}.

The absorptions of the liquefied material are much higher than those of the initial material, probably due to the air between the solid samples and ATR crystal resulting in a weaker absorbance signal for the initial material, and also due to the infrared radiation decrease with penetration depth [56].

The FTIR spectra of the original and liquified material from hydrolysed SCS at 170 °C are presented in Figure 6.

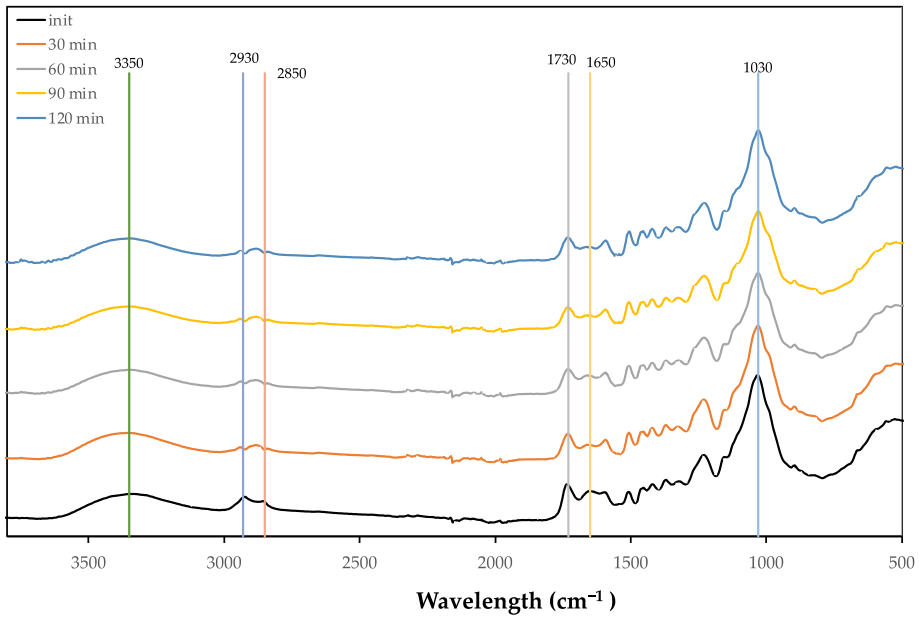

Figure 6. FTIR spectra of the original and liquified material from hydrolysed SCS at 170 °C.

The clearest change between the initial material and the hydrolysed material is the high increase in the OH band at around 3350 cm^{-1}, although there is no visible increase over the pre-hydrolysis time. This occurred at both 170 °C (Figure 6) and 160 °C (Figure 5). There is a shifting of the 2850 cm^{-1} peak to higher wavelengths at both temperatures, even starting at a 30 min reaction time. In relation to the 1730 cm^{-1} peak of non-conjugated C=O links, there seems to be an initial decrease for both temperatures, followed by an increase at 170 °C. This shows that several reactions are occurring at the same time during pre-hydrolysis. The C=O linkage has a strong absorption between 1750 and 1700 cm^{-1}, varying in accordance to the functional groups, with higher wavenumbers for aldehyde (1740–1720 cm^{-1}) followed by ketones (1725–1705 cm^{-1}) and carboxylic acids (1725–1700 cm^{-1}) [55]. Contrary to this, the peak at around 1600 cm^{-1} increased for the 30 min reaction, decreasing afterwards. This peak is mostly associated with benzene ring stretching vibrations, which could corroborate the wet analysis that shows that lignin increases in the residue, which means that there is a percentual decrease in the liquid. There was an increase followed by a decrease in the peak at around 1367 cm^{-1}. This decrease was not observed at 160 °C. Somewhat similar

behaviour was observed for the peak at around 1230 cm^{-1}. A new shoulder appeared at 1060 cm^{-1} in the 1030 cm^{-1} band that was mainly attributed to the C-O stretching in holocellulose [57].

4. Conclusions

The chemical characterization of the sweet cherry seeds shows that this material has several components that allow the recovery of its residue. The chemical composition of samples that underwent pre-hydrolysis tests showed that, with an increase in time (from 30 to 180 min) and temperature (from 160 °C to 170 °C), there was an increase in the amounts of lignin and α-cellulose. In the initial sample, hemicelluloses represented the major component, while, after pre-hydrolysis, lignin and cellulose were the main polymers. The high lignin content shows that this residue has enormous potential to produce adhesives or rigid polyurethane foams with high mechanical resistance.

FTIR analysis showed that there were significant changes in the spectra from the initial material, solid residue, and liquefied material, the clearest being the increased OH band in the liquefied material, which was probably due to the solubilized hemicelluloses. The changes in the FTIR spectra of both the solid residue and the liquefied material throughout the pre-hydrolysis show that there were a lot of different reactions occurring at the same time, some increasing and others decreasing the same functional groups, making it difficult to track the changes over the pre-hydrolysis steps.

Potassium was the most representative inorganic compound, followed by calcium and phosphorous.

Author Contributions: Conceptualization, L.C.-L. and B.E.; methodology, L.C.-L., Y.D. and B.E.; formal analysis, L.C.-L. and Y.D.; investigation, L.C.-L., Y.D. and B.E.; resources, L.C.-L., Y.D., I.D., J.F., A.F., R.G. and B.E.; writing—original draft preparation, Y.D.; writing—review and editing, L.C.-L., R.G. and B.E.; supervision, L.C.-L. All authors have read and agreed to the published version of the manuscript.

Funding: This work is funded by National Funds through the FCT—Foundation for Science and Technology. I.P. within the scope of the project Ref UIDB/00681/2020 (CERNAS) and Ref UIDB/05507/2020 (CI&DEI).

Data Availability Statement: Not applicable.

Acknowledgments: We would like to thank the CERNAS and CI&DEI Research Centre and the Polytechnic Institute of Viseu for their support and the PROJ/IPV/ID&I/021, "Valorização de resíduos: potencial de aproveitamento do caroço de cereja (VALCER)" pela Bolsa de Investigação de Yulia.

Conflicts of Interest: The authors declare no conflict of interest.

References

1. Proietti, S.; Moscatello, S.; Villani, F.; Mecucci, F.; Walker, R.P.; Famiani, F.; Battistelli, A. Quality and Nutritional Compounds of *Prunus cerasus* L. Var. Austera Fruit Grown in Central Italy. *HortScience* **2019**, *54*, 1005–1012. [CrossRef]
2. Švarc-Gajić, J.; Cerdà, V.; Clavijo, S.; Suárez, R.; Mašković, P.; Cvetanović, A.; Delerue-Matos, C.; Carvalho, A.P.; Novakov, V. Bioactive compounds of sweet and sour cherry stems obtained by subcritical water extraction. *J. Chem. Technol. Biotechnol.* **2018**, *93*, 1627–1635. [CrossRef]
3. Publication | Stone Fruit: World Markets and Trade | ID: 0g354f20t | USDA Economics, Statistics and Market Information System. Available online: https://usda.library.cornell.edu/concern/publications/0g354f20t?locale=en (accessed on 29 August 2021).
4. Portal Do INE. Available online: https://www.ine.pt/xportal/xmain?xpid=INE&xpgid=ine_publicacoes&PUBLICACOESpub_boui=358629204&PUBLICACOESmodo=2 (accessed on 7 August 2021).
5. de Oliveira, T.S. O Marketing da Cereja da Cova da Beira. Ph.D. Thesis, University of Beira Interior, Covilhã, Portugal, 2015. Volume 73.
6. Produtos Tradicionais de Qualidade na Região Centro. Available online: https://ptqc.drapc.gov.pt/documentos/cereja_cova_beira.htm (accessed on 14 November 2021).
7. Delgado, J.; Terrón, M.P.; Garrido, M.; Barriga, C.; Paredes, S.D.; Espino, J.; Rodríguez, A.B. Systemic Inflammatory Load in Young and Old Ringdoves Is Modulated by Consumption of a Jerte Valley Cherry-Based Product. *J. Med. Food* **2012**, *15*, 707–712. [CrossRef] [PubMed]

8. McCune, L.M.; Kubota, C.; Stendell-Hollis, N.R.; Thomson, C.A. Cherries and Health: A Review. *Crit. Rev. Food Sci. Nutr.* **2010**, *51*, 1–12. [CrossRef] [PubMed]
9. Martínez-Esplá, A.; Zapata, P.J.; Valero, D.; García-Viguera, C.; Castillo, S.; Serrano, M. Preharvest Application of Oxalic Acid Increased Fruit Size, Bioactive Compounds, and Antioxidant Capacity in Sweet Cherry Cultivars (*Prunus avium* L.). *J. Agric. Food Chem.* **2014**, *62*, 3432–3437. [CrossRef]
10. Callahan, A.M.; Dardick, C.; Scorza, R. Characterization of 'Stoneless': A Naturally Occurring, Partially Stoneless Plum Cultivar. *J. Am. Soc. Hortic. Sci.* **2009**, *134*, 120–125. [CrossRef]
11. Aires, A.; Carvalho, R.; Saavedra, M.J. Valorization of solid wastes from chestnut industry processing: Extraction and optimization of polyphenols, tannins and ellagitannins and its potential for adhesives, cosmetic and pharmaceutical industry. *Waste Manag.* **2016**, *48*, 457–464. [CrossRef]
12. Ventorino, V.; Parillo, R.; Testa, A.; Viscardi, S.; Espresso, F.; Pepe, O. Chestnut green waste composting for sustainable forest management: Microbiota dynamics and impact on plant disease control. *J. Environ. Manag.* **2016**, *166*, 168–177. [CrossRef]
13. Yılmaz, F.M.; Görgüç, A.; Karaaslan, M.; Vardin, H.; Bilek, S.E.; Uygun, Ö.; Bircan, C. Sour Cherry By-products: Compositions, Functional Properties and Recovery Potentials—A Review. *Crit. Rev. Food Sci. Nutr.* **2019**, *59*, 3549–3563. [CrossRef]
14. Bernardo-Gil, G.; Oneto, C.; Antunes, P.; Rodrigues, M.F.; Empis, J.M. Extraction of lipids from cherry seed oil using supercritical carbon dioxide. *Eur. Food Res. Technol.* **2001**, *212*, 170–174. [CrossRef]
15. Duman, G.; Okutucu, C.; Ucar, S.; Stahl, R.; Yanik, J. The slow and fast pyrolysis of cherry seed. *Bioresour. Technol.* **2011**, *102*, 1869–1878. [CrossRef] [PubMed]
16. Petrov, N.; Budinova, T.; Razvigorova, M.; Minkova, V.; Vigouroux, R.; Björnbom, E. Preparation of activated carbons from cherry stones, apricot stones and grape seeds for removal of metal ions from water. In Proceedings of the 2nd Olle Indstorm Symposium on Renewable Energy-Bioenergy, Royal Institute of Technology, Stockholm, Sweden, 9–11 June 1999; pp. 46–550.
17. González, J.F.; Encinar, J.M.; Canito, J.L.; Sabio, E.; Chacón, M. Pyrolysis of cherry stones: Energy uses of the different fractions and kinetic study. *J. Anal. Appl. Pyrolysis* **2003**, *67*, 165–190. [CrossRef]
18. González-Domínguez, J.M.; Fernández-González, M.C.; Alexandre-Franco, M.; Gómez-Serrano, V. How does phosphoric acid interact with cherry stones? A discussion on overlooked aspects of chemical activation. *Wood Sci. Technol.* **2018**, *52*, 1645–1669. [CrossRef]
19. Kumari, D.; Singh, R. Pretreatment of lignocellulosic wastes for biofuel production: A critical review. *Renew. Sustain. Energy Rev.* **2018**, *90*, 877–891. [CrossRef]
20. Roy, R.; Rahman, M.S.; Raynie, D.E. Recent advances of greener pretreatment technologies of lignocellulose. *Curr. Res. Green Sustain. Chem.* **2020**, *3*, 100035. [CrossRef]
21. Laurichesse, S.; Avérous, L. Chemical modification of lignins: Towards biobased polymers. *Prog. Polym. Sci.* **2014**, *39*, 1266–1290. [CrossRef]
22. Wang, S.; Liu, W.; Yang, D.; Qiu, X. Highly resilient lignin-containing polyurethane foam. *Ind. Eng. Chem. Res.* **2018**, *58*, 496–504. [CrossRef]
23. Li, H.-Q.; Shao, Q.; Luo, H.; Xu, J. Polyurethane foams from alkaline lignin-based polyether polyol. *J. Appl. Polym. Sci.* **2016**, *133*. [CrossRef]
24. Haridevan, H.; Evans, D.A.; Ragauskas, A.J.; Martin, D.J.; Annamalai, P.K. Valorisation of technical lignin in rigid polyurethane foam: A critical evaluation on trends, guidelines and future perspectives. *Green Chem.* **2021**, *23*, 8725–8753. [CrossRef]
25. Flôres, C.C.; Rufino, T.d.C.; Oliveira, M.P. Effect of Kraft lignin and palm kernel oil as substitutes of petroleum-based polyols on the properties of viscoelastic polyurethane foams. *J. Polym. Res.* **2021**, *28*, 1–15. [CrossRef]
26. Cinelli, P.; Anguillesi, I.; Lazzeri, A. Green synthesis of flexible polyurethane foams from liquefied lignin. *Eur. Polym. J.* **2013**, *49*, 1174–1184. [CrossRef]
27. Ghaffar, S.H.; Fan, M. Lignin in straw and its applications as an adhesive. *Int. J. Adhes. Adhes.* **2014**, *48*, 92–101. [CrossRef]
28. Bertaud, F.; Tapin-Lingua, S.; Pizzi, A.; Navarrete, P.; Petit-Conil, M. Development of green adhesives for fibreboard manufacturing, using tannins and lignin from pulp mill residues. *Cell. Chem. Technol.* **2012**, *46*, 449–455.
29. Lee, S.J.; Kim, H.J.; Cho, E.J.; Song, Y.; Bae, H.-J. Isolation and characterization of lignin from the oak wood bioethanol production residue for adhesives. *Int. J. Biol. Macromol.* **2015**, *72*, 1056–1062. [CrossRef] [PubMed]
30. Olivares, M.; Guzmán, J.A.; Natho, A.; Saavedra, A. Kraft lignin utilization in adhesives. *Wood Sci. Technol.* **1988**, *22*, 157–165. [CrossRef]
31. Mansouri, N.-E.E.; Pizzi, A.; Salvado, J. Lignin-based polycondensation resins for wood adhesives. *J. Appl. Polym. Sci.* **2007**, *103*, 1690–1699. [CrossRef]
32. Pizzi, A. Recent developments in eco-efficient bio-based adhesives for wood bonding: Opportunities and issues. *J. Adhes. Sci. Technol.* **2006**, *20*, 829–846. [CrossRef]
33. Hamaguchi, M.; Kautto, J.; Vakkilainen, E. Effects of hemicellulose extraction on the kraft pulp mill operation and energy use: Review and case study with lignin removal. *Chem. Eng. Res. Des.* **2013**, *91*, 1284–1291. [CrossRef]
34. Liu, Z.; Fatehi, P.; Sadeghi, S.; Ni, Y. Application of hemicelluloses precipitated via ethanol treatment of pre-hydrolysis liquor in high-yield pulp. *Bioresour. Technol.* **2011**, *102*, 9613–9618. [CrossRef]
35. Al-Dajani, W.W.; Tschirner, U.W. Pre-extraction of hemicelluloses and subsequent kraft pulping Part I: Alkaline extraction. *Bioprod. Biosyst. Eng.* **2008**, *7*, 3–8.

36. Helmerius, J.; von Walter, J.V.; Rova, U.; Berglund, K.A.; Hodge, D.B. Impact of hemicellulose pre-extraction for bioconversion on birch Kraft pulp properties. *Bioresour. Technol.* **2010**, *101*, 5996–6005. [CrossRef] [PubMed]
37. Sidiras, D.K.; Koukios, E.G. Acid saccharification of ball-milled straw. *Biomass* **1989**, *19*, 289–306. [CrossRef]
38. Zhu, J.Y.; Pan, X.; Zalesny, R.S. Pretreatment of woody biomass for biofuel production: Energy efficiency, technologies, and recalcitrance. *Appl. Microbiol. Biotechnol.* **2010**, *87*, 847–857. [CrossRef] [PubMed]
39. Saeed, A.; Jahan, M.S.; Li, H.; Liu, Z.; Ni, Y.; van Heiningen, A. Mass balances of components dissolved in the pre-hydrolysis liquor of kraft-based dissolving pulp production process from Canadian hardwoods. *Biomass Bioenergy* **2012**, *39*, 14–19. [CrossRef]
40. Liu, C.; Wyman, C.E. Partial flow of compressed-hot water through corn stover to enhance hemicellulose sugar recovery and enzymatic digestibility of cellulose. *Bioresour. Technol.* **2005**, *96*, 1978–1985. [CrossRef] [PubMed]
41. Li, H.; Saeed, A.; Jahan, M.S.; Ni, Y.; van Heiningen, A. Hemicellulose removal from hardwood chips in the pre-hydrolysis step of the kraft-based dissolving pulp production process. *J. Wood Chem. Technol.* **2010**, *30*, 48–60. [CrossRef]
42. TAPPI. 264 om-97. In *Preparation of Wood in Chemical Analysis*; TAPPI: Peachtree Corners, GA, USA, 1997.
43. TAPPI. 211 om–93. In *Ash in Wood, Pulp, Paper and Paperboard: Combustion at 525 °C*; TAPPI: Peachtree Corners, GA, USA, 1993.
44. Prozil, S.O.; Evtuguin, D.V.; Lopes, L.P.C. Chemical composition of grape stalks of Vitis vinifera L. from red grape pomaces. *Ind. Crops Prod.* **2012**, *35*, 178–184. [CrossRef]
45. Neto, C.P.; Seca, A.; Fradinho, D.; Coimbra, M.A.; Domingues, F.; Evtuguin, D.; Silvestre, A.; Cavaleiro, J.A.S. Chemical composition and structural features of the macromolecular components of Hibiscus cannabinus grown in Portugal. *Ind. Crops Prod.* **1996**, *5*, 189–196. [CrossRef]
46. Browning, B.L. *Methods of Wood Chemistry Volume I & II*; John Wiley & Sons: Hoboken, NJ, USA, 1967.
47. Venegas-Gomez, A.; Gomez-Corzo, M.; Macías-García, A.; Carrasco-Amador, J.P. Charcoal obtained from cherry stones in different carbonization atmospheres. *J. Envirom. Chem. Eng.* **2020**, *8*, 103561. [CrossRef]
48. Kamel, B.S.; Kakuda, Y. Characterization of the seed oil and meal from apricot, cherry, nectarine, peach and plum. *J. Am. Oil Chem. Soc.* **1992**, *69*, 492–494. [CrossRef]
49. García-Aguilar, L.; Rojas-Molina, A.; Ibarra-Alvarado, C.; Rojas-Molina, J.; Vázquez-Landaverde, P.; Luna-Vázquez, F.; Zavala-Sánchez, M. Nutritional Value and Volatile Compounds of Black Cherry (*Prunus serotina*) Seeds. *Molecules* **2015**, *20*, 3479–3495. [CrossRef] [PubMed]
50. Mendes, C.V.T.; Carvalho, M.; Baptista, C.; Rocha, J.M.S.; Soares, B.I.G.; Sousa, G.D.A. Valorisation of hardwood hemicelluloses in the kraft pulping process by using an integrated biorefinery concept. *Food Bioprod. Process.* **2009**, *87*, 197–207. [CrossRef]
51. Colodette, J.L.; Longue, D., Jr.; Pedrazzi, C.; Oliveira, R.C.; Gomide, J.L.; Gomes, F.J. Pulpability and bleachability of xylan-depleted eucalyptus wood chips. *Ind. Eng. Chem. Res.* **2011**, *50*, 1847–1852. [CrossRef]
52. Al-Dajani, W.W.; Tschirner, U.W.; Jensen, T. Pre-extraction of hemicelluloses and subsequent kraft pulping Part II: Acid-and autohydrolysis. *Bioprod. Biosyst. Eng.* **2009**, *8*, 30–37.
53. Esteves, B.; Marques, A.V.; Domingos, I.; Pereira, H. Chemical changes of heat treated pine and eucalypt wood monitored by FTIR. *Maderas Cienc. Tecnol.* **2013**, *15*, 245–258. [CrossRef]
54. Coates, J. Interpretation of Infrared Spectra, a Practical Approach. In *Encyclopedia of Analytical Chemistry*; John Wiley & Sons: Hoboken, NY, USA, 2000.
55. Esteves, B.; Cruz-Lopes, L.; Ferreira, J.; Domingos, I.; Nunes, L.; Pereira, H. Optimizing Douglas-fir bark liquefaction in mixtures of glycerol and polyethylene glycol and KOH. *Holzforschung* **2018**, *72*, 25–30. [CrossRef]
56. Jelle, B.P.; Nilsen, T.-N.; Hovde, P.J.; Gustavsen, A. Accelerated climate aging of building materials and their characterization by Fourier transform infrared radiation analysis. *J. Build. Phys.* **2012**, *36*, 99–112. [CrossRef]
57. Lao, W.; Li, G.; Zhou, Q.; Qin, T. Quantitative analysis of biomass in three types of wood-plastic composites by FTIR spectroscopy. *BioResources* **2014**, *9*, 6073–6086. [CrossRef]